Naval Information Warfare Center PACIFIC

TECHNICAL REPORT 3284
JULY 2022

Quadrature Compensation and Demodulation Phase Reference Selection for FM Accelerometers

Andrew Sabater
NIWC Pacific

Naval Information Warfare Center (NIWC) Pacific
San Diego, CA 92152-5001

This page is intentionally blank.

TECHNICAL REPORT 3284
JULY 2022

Quadrature Compensation and Demodulation Phase Reference Selection for FM Accelerometers

Andrew Sabater
NIWC Pacific

Administrative Notes:
This report was approved through the Release of Scientific and Technical Information (RSTI) process in June 2022 and formally published in the Defense Technical Information Center (DTIC) in July 2022.

NIWC Pacific
San Diego, CA 92152-5001

NIWC Pacific
San Diego, California 92152-5001

A. D. Gainer, CAPT, USN
Commanding Officer

W. R. Bonwit
Executive Director

ADMINISTRATIVE INFORMATION

The work described in this report was performed by the Nonlinear Dynamics and Materials Research Branch (71780) of the Basic and Applied Research Division, Naval Information Warfare Center Pacific (NIWC Pacific), San Diego, CA. The NIWC Pacific In-House Laboratory Independent Research (ILIR) Program provided funding for this Basic Research project.

Released by
John deGrassie, Division Head
Basic and Applied Research

Under authority of
Carly Jackson, Department Head
Cyber, Science and Technology

ACKNOWLEDGMENTS

Editor: RJP

EXECUTIVE SUMMARY

Inertial navigation provides a means to operate independent of external signals such as the ones providedby a GNSS (global navigation satellite system). The estimated position provided by inertial navigation willdrift for a variety of reasons internal and external to the utilized sensors, but removing bias drift from the accelerometers can significantly mitigate this issue. This work aims to address this issue. The methods described herein document means to select the offset phase of frequency modulated (FM) accelerometers that can both be implemented in a real-time fashion and be used with a simple model to improve long-termstability. It provides improvements upon prior work that utilized autoregressive modeling, so this method isexpected to be suitable for nonstationary acceleration. The method is based on an observation in experiments that found orthogonal channels to be highly correlated. Utilizing this approach, bias instabilitywas improved by more than two orders of magnitude. However, as the bias instability was recorded at the longest measurement period, by increasing the measurement length, it is expected that the actual bias instability is lower. Future work to determine this as well as other areas are outlined at the end of the report.

This page is intentionally blank.

CONTENTS

Figures

This page is intentionally blank.

1. INTRODUCTION

Inertial navigation provides a means to navigate independent of externals signals provided by a GNSS (global navigation satellite system). This form of navigation typically relies upon the integration of measurements from inertial sensors such as accelerometers and gyroscopes with a navigation filter to estimate position, velocity, and attitude. As accelerometers are capable of detecting acceleration relative to gravity, a model of local gravity is needed to estimate the actual acceleration. The position estimate provided by inertial navigation can be degraded for a variety of factors internal and external to these sensors. Internal factors can include Gaussian noise processes associated with electronics of the sensors and a slow drift due to temperature variations or packaging material aging. External factors include initialization errors (an error in the initial estimate for position, velocity or attitude) or deflection of vertical (DOV) errors associated with modeling errors for local gravity [1]. Accelerometer bias and DOV error effectively give rise to the same effect–for periods less than one eighth of the Schuler cycle (about 11 minutes), these errors contribute the most to the estimated position drift [1]. This work aims to address both of these issues. By creating very stable accelerometers, position drift due to bias changes can be mitigated. Moreover, a pair of stable accelerometers could be used to create a strapdown (i.e. rigidly mounted to a vehicle) gravity gradiometer. With a gravity gradiometer along with an inertial measurement unit, it is possible to estimate local gravity [2]. Provided that local gravity maps are accurate, map-matching methods that utilize a gravity gradiometer can provide a means to bound the position drift associated with utilizing just inertial sensors for navigation [3].

This report builds upon and provides improvements relative to prior results [4]. The first section discusses a theoretical model for the time-switched frequency modulated (FM) accelerometer. An overview of the operating principle of the device is presented. In contrast to prior work that sought to enhance sensitivity by using as large as possible voltages, the model voltages were selected to more closely align with experiments. Aspects related to the needed control systems and signal processing are introduced including the standard or currently accepted approach for tuning the phase offset of the phase reference. The next section discusses the experimental setup. Several important improvements such as temperature control are documented. Using the improved experimental setup, work related to data acquisition, processing, and analysis is reported. To mitigate issues related to frequency locking with the modulation reference, a means to extract the reference from the demodulated frequency is used. Based on experiments that found strong correlations between the in-phase and out-of-phase channels, a novel means to select the offset phase of the phase reference and compensate the accelerometer's response is demonstrated. In contrast to prior works [4], autoregressive modeling was not needed. As autoregressive modeling typically works well when the signal can be decomposed into stationary components or known trends, the proposed method is expected to work well when the acceleration signal is nonstationary. Moreover, this method provides a means to select the phase offset that could be implemented in an online fashion, minimizing calibration and could be useful to address issues related to turn on and off bias repeatability. At the longest integration time for the experiment configured to be insensitive to ambient vibrations, bias instability was reduced by more than two orders of magnitude to 1.341 μg at about 14,000 sec. However, as the Allan deviation is not limited by long-term drift or 1/f noise processes, it is very possible that the bias instability is lower. Future work is discussed in the final section. Planned experiments include determining the lower limit for bias instability and determining the fundamental source of drift in the sensor's uncompensated outputs. Future improvements to the accelerometer include implementing resonators with a higher scale factor, improving the electronics, and using optical methods to detect the resonator's motion.

This page is intentionally blank.

2. ACCELEROMETER MODEL

The model presented is this work is based on the one presented in [4]. See that report for the design, layout, and simulation approach. The heart of a single-resonator, time-switched accelerometer is a tuning fork-like structure with an associated anti-phase mode and an in-phase mode that is sensitive to acceleration. A positive feedback loop is implemented to sustain the oscillations of the anti-phase mode at a constant amplitude. To compensate for damping of the anti-phase mode, in experiments, an automatic gain control circuit is needed to maintain a constant amplitude. However, in simulation, if the anti-phase mode is assumed to be undamped, the amplitude of the anti-phase model will stay constant.

To introduce a sensitivity to acceleration, two pairs of electrodes are aligned to the in-phase mode. When a given pair of electrodes are polarized, due to in-phase motion caused by acceleration, the frequency of the anti-phase mode decreases as the in-phase displacement (relative to the active electrode) decreases and the frequency of the anti-phase mode increases as the relative in-phase displacement increases. By using out-of-phase voltages applied to these pairs of electrodes, a differential frequency-based means to estimate acceleration can be provided by demodulating the oscillator's frequency and then subsequently demodulating at the modulation frequency. The phase of last demodulation reference is important as the in-phase (IP) response is sensitive to acceleration and the out-of-phase (OOP) response is not. To compensate for delays for example with the electronics, frequency demodulation, etc., common practice is to adjust the phase reference such that the in-phase response is maximally sensitive to acceleration. However, as will be shown in section 4, the selection of the phase reference can be made to optimize other accelerometer metrics.

There are notable modifications or differences between this model and other work. Relative to the experiments, the modulation reference was selected to be much higher than the one used in experiments (100 Hz vs. 4 Hz) as it decreases the time needed to complete the simulation. Relative to prior modeling, the applied voltages are much lower due to noise observed with large bias voltages in the experiments (30 V vs. 80 V). While the use of bias voltages near the pull-in voltage provide a means to maximize scale factor, low-frequency noise from the bias voltage is aliased into the side-bands near the oscillator's operating frequency [5]. Besides these modifications, the same model parameters based on the nominal layout of the device was used. Over-etching was expected and observed with fabricated dies. The most significant impact of over-etching is the actual scale factor should be slightly lower than the one based on the nominal layout.

Shown in Figure 1 is the IP and OOP response of the accelerometer before the phase reference was adjusted to maximize the sensitivity of the IP response. In this case, the scale factor, or the slope of the output with respect to acceleration, of the OOP response is greater than the IP response. As in the simulation, there are no delays associated with the electronics, the primary source of delay is associated with the phase locked loop used for frequency demodulation. To compensate for this delay, a root-solving algorithm was used to find the phase delay that would result in a zero OOP scale factor. This compensated response is shown in Figure 2. Thus, based on these results, one could suggested that a particular phase delay could be used to decouple to the IP response from the OOP response. However, based on experimental results, the IP and OOP responses are in general highly correlated.

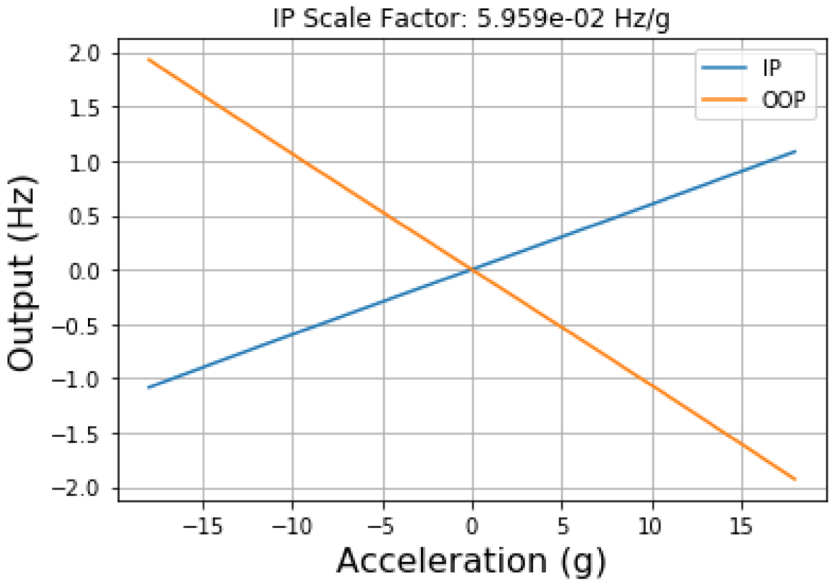

Figure 1. The in-phase (IP) and out-of-phase (OOP) first-harmonic response before adjusting the phase reference to maximize the IP sensitivity.

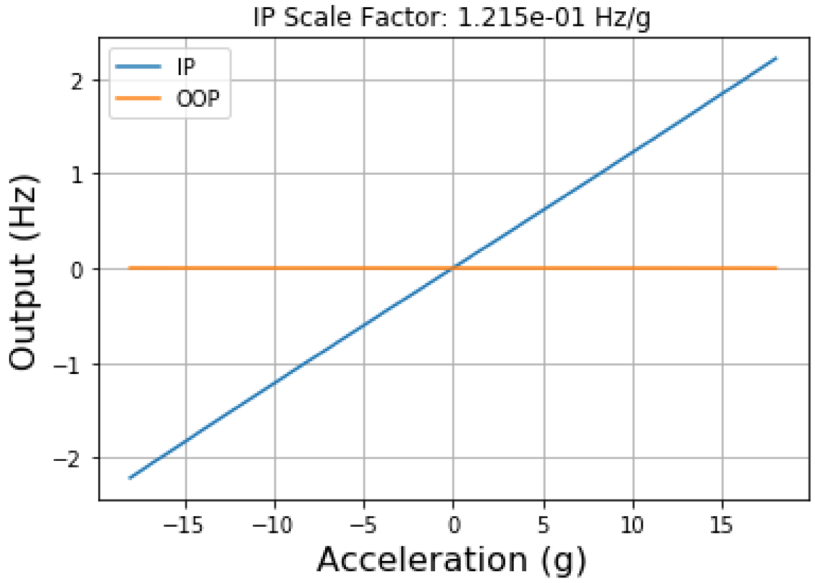

Figure 2. The in-phase (IP) and out-of-phase (OOP) first-harmonic response after adjusting the phase reference to maximize the IP sensitivity.

3. EXPERIMENTAL SETUP

The primary results in this work have been experimentally demonstrated. Current efforts are focused on developing the theoretical basis. The experimental setup is based on the one presented in [4] with a few important modifications. To mitigate issues associated with packaging stress, dies were bonded at room temperature using a cyanoacrylate-based epoxy. As shown in Figure 3, to enable active temperature control, in the chip carrier (Spectrum Semi LCC04438), the dies were co-packaged with wire bondable power resistors (Vishay PWB7500AJKGNHT5) and an resistance temperature device (RTD) (Jumo 0064779500647795). By placing the heating elements and temperature sensor close to the accelerometer resonator, errors associated with a thermal gradient can be minimized. To further help to minimize package stress issues associated with elevated temperatures, wire bonding was also done at ambient temperature.

As the resonator needs to be placed in a vacuum to minimize viscous damping, an interface electronics board was placed inside a vacuum chamber with electrical feedthroughs. See Figure 10 of [4] for a schematic. Important updates were new interface electronic boards were fabricated with the needed modifications for components for temperature control and a socket that is compatible with the chip carrier. To enable closed-loop temperature control, an Adafruit PT1000 RTD Temperature Sensor Amplifier that contains a MAX31865 was used for a four-probe resistance measurement to estimate temperature. To improve sensitivity, the reference resistance was decreased from 4 KOhm to 2 KOhm resulting in the nominal sensitivity being halved to about 0.016 C. A Linduino, a microcontroller that is compatible with Linear Technology and now Analog Devices developments kits and utilizes the Arduino Uno development platform, was used to read the SPI output of the MAX31865. A digital PI (proportional-integral) control loop was implemented to control a DAC that is connected to the power resistors on the chip carrier. Due to the thermal insulation of the vacuum chamber, when the interface electronics board is on, the temperature of the chamber settles to above 30 C. As this type of temperature control cannot remove heat, the setpoint of the controller was set to about 40 C. After settling, the temperature controller is able to maintain the temperature at 40.01 +/- 0.01 C (mean +/- standard deviation).

To provide a crude means to estimate scale factor with two data points, a leveling mount was used to hold the interface electronics board vertical (to measure 1 g) or the board was placed horizontally (to measure 0 g). To switch between these two measurement states, the vacuum chamber had to be pressurized and opened. In prior work it was assumed that the 0 g bias was insignificant and that the scale factor could be estimated from the 1 g measurement. This work attempts to rectify this issue. The theoretical scale from section 2 also provides additional context for the actual scale factor.

A block diagram of the electronics subsystems is shown in Figure 4. To sustain the oscillations of the anti-phase mode, a negative feedback loop was implemented. To maintain the amplitude of the anti-phase mode at a constant value, a proportional-integral analog automatic gain control circuit was implemented that adjusts the supply voltage of the inverter/buffer that drives the anti-phase mode. The frequency of the anti-phase mode is demodulated using a Red Pitaya STEMlab125-14 [6]. As compared to the electronics setup in prior work, a few changes have been made. As noted earlier, a closed-loop temperature control system was implemented to maintain the device at 40 C. A function generator with a differential output was connected to the in-phase electrodes that modulate acceleration sensitivity. The bias voltage applied to the resonator was 30 V. To boost the output of the function generator such that the maximum voltage applied to the in-phase electrodes matched the bias voltage, a piezo amplifer was used. In the past this function generator was also connected to the Red Pitaya so that the phase reference could be recorded. However, the software phase-locked loop (PLL) implemented on the Red Pitaya had issues with locking to the low-frequency signal, so the phase reference was extracted by filtering the demodulated frequency. This is discussed in greater detail in the section 4.

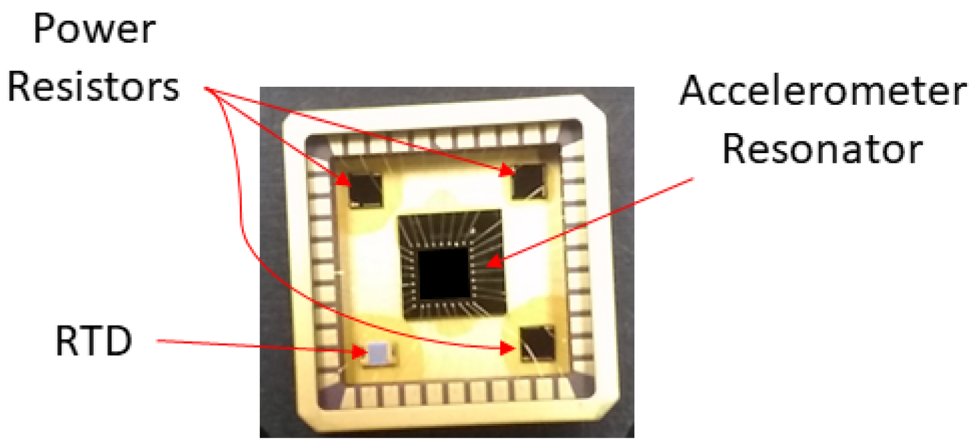

Figure 3. The accelerometer resonator bonded to the chip carrier with the components needed for closed-loop temperature control.

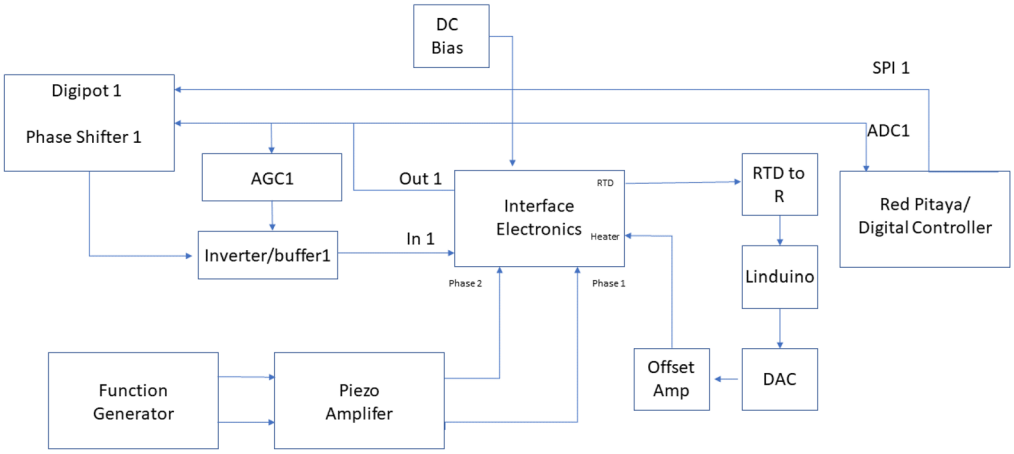

Figure 4. The electronics block diagram with the control system needed for closed-loop temperature control.

4. SIGNAL PROCESSING AND DATA ANALYSIS

An integral aspect of getting the most out of an FM inertial sensor is optimizing the signal processing and control systems. In prior work, an attenuated version of one of the signals used to modulate acceleration sensitivity was connected to the second ADC channel on the Red Pitaya. This worked poorly as the implemented software PLL would not maintain a constant lock during tests as the settings for the loop filter were incorrect. However, it is possible to extract the needed reference from the demodulated frequency. By effectively bandpass filtering the demodulated frequency centered at the modulation frequency (4 Hz in this work), the needed reference can be extracted. Shown in blue in Figure 5 is the power spectral density (PSD) of the demodulated frequency of the accelerometer when setup to detect at approximately 0 g. The two main peaks are at 4 and 8 Hz. Shown in orange is the PSD of the bandpass filtered signal to extract the reference at 4 Hz. To use this signal for subsequent processing, it was then scaled and a tuned software PLL was able to extract the reference.

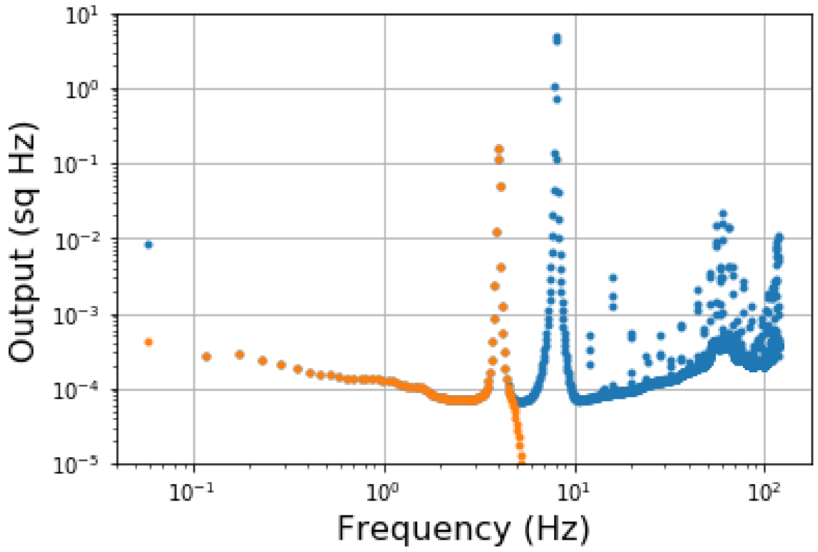

Figure 5. Power spectral density (PSD) of the demodulated frequency when the accelerometer is setup to measure approximately 0 g is shown in blue. The bandpassed filtered signal used to extract the phase reference is shown in orange.

The standard approach for selecting the phase offset for FM accelerometers is to maximize the IP scale factor and in turn improve sensitivity. One could justify this approach based on the assumption that the OOP channel provides no useful information after the phase offset was tuned to maximize IP scale factor as these channels should be orthogonal. To test this assumption, shown in Figure 6 are the mean values of the IP and OOP channels for the accelerometer setup to measure approximately -1 g for different phase offset values. Note that the extremum of the IP channel corresponds to a zero of the OOP channel. Shown in Figure 7 is the correlation coefficient (R value) and slope between the IP and OOP channels for different phase offset values. Note that the magnitude of the correlation coefficient is nearly one for most values of the phase offset and that a rapid transition to zero occurs for phase values where the slope is about zero. Thus, in general, the IP and OOP channel are highly correlated. Based on prior work, with a highly correlated signal that can be used to observe bias drift, a simple linear model can be implemented to improve long-term stability [4].

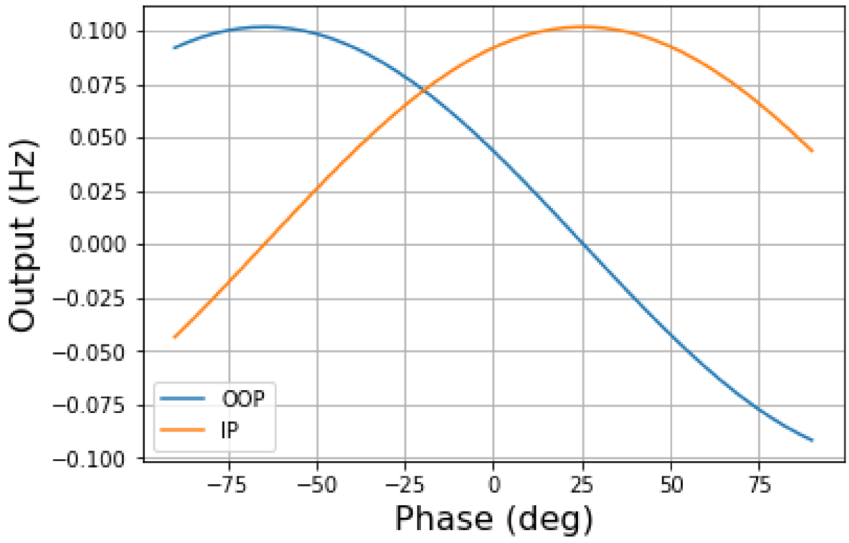

Figure 6. The mean value of the IP and OOP channels versus phase when setup to measure -1 g.

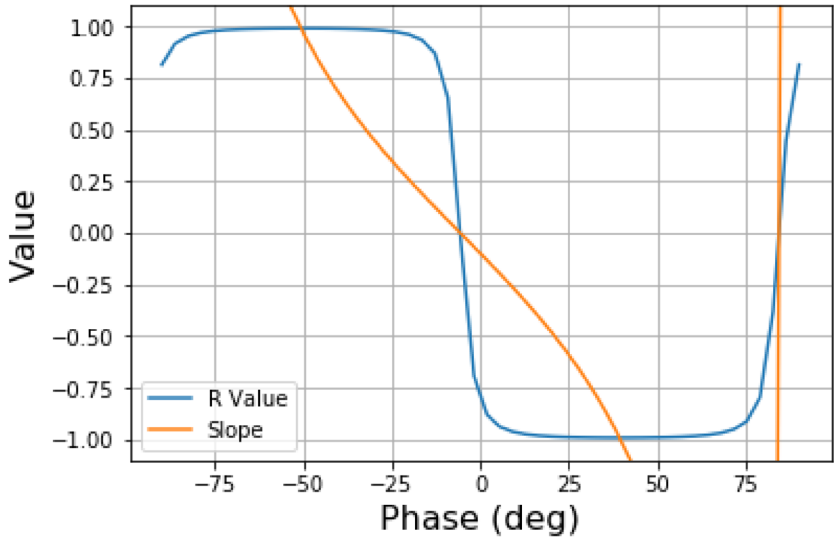

Figure 7. The correlation coefficient and slope between the IP and OOP channels versus phase when setup to measure -1 g. A slope of -1 occurs for a phase of 39.025°.

Due to the curvature of the correlation coefficient versus phase offset relationship, finding the extremum can be challenging and simple numerical methods at best slowly converge. Interesting, note that the cases when the magnitude of the correlation coefficient is near one, the magnitude of the slope is near one. This work proposes selecting the offset phase such that the magnitude of the slope is near one. While providing an easy point to converge to when post-processing data, online methods that in a closed-loop fashion estimate the slope and adjust the phase to maintain this relationship could be implemented. This simple method dramatically improves long-term stability at the slight cost of decreasing the IP scale factor.

Shown in Figure 8 is the IP response to a -1 g input with the phase reference selected such that the slope between the IP and OOP channels is -1. The compensated response was created by assuming a simple

linear model with a slope of -1. To quantify the various noise processes that impact each response, the Allan deviation of the time series are shown in Figure 9. While the uncompensated response slowly drifts, the compensated response is Gaussian for all but the shortest and longest averaging times.

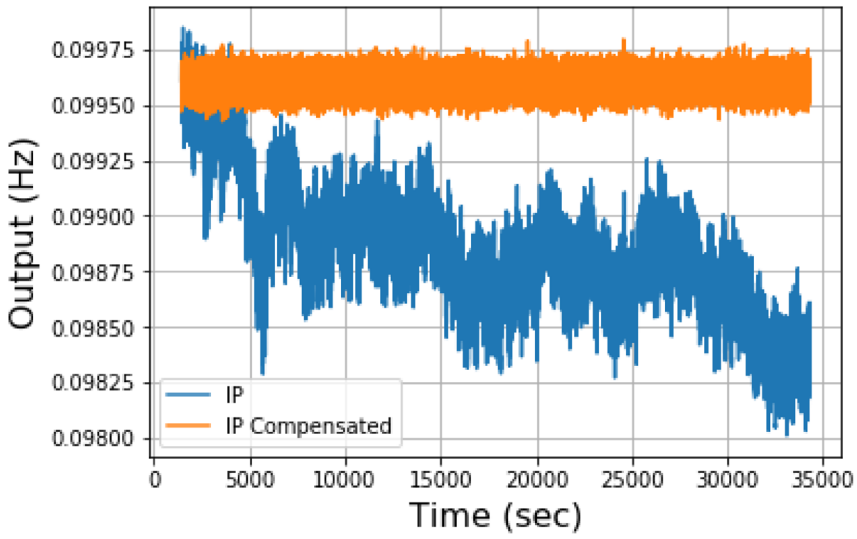

Figure 8. Time series of the IP and IP channel compensated with the OOP channel when setup to measure -1 g. The mean and standard deviation of the IP compensated response is 9.960$\times 10^{-2}$ +/- 0.004$\times 10^{-2}$ Hz.

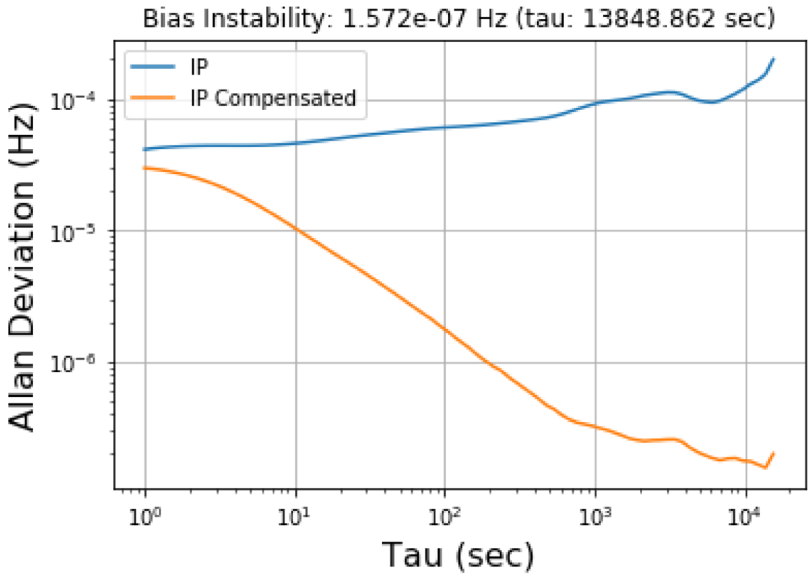

Figure 9. Allen deviation of the IP and IP channel compensated with the OOP channel when setup to measure -1 g.

To approximately estimate the scale factor to convert the frequency output to acceleration units and assess if the slope relationship is stable, the experiment was repeated with a nearly 0 g input. Note that to transition between measurement setups, the power for the electronics had to be turned off, the vacuum

chamber was pressurized, the measurement configuration was adjusted, the vacuum chamber was evacuated, and then the electronics were turned back on, so these tests are sensitive to issues related to on/off bias repeatability issues. There was approximately a four day period between the two tests shown in this report. Figure 10 shows the mean values of the IP and OOP channels versus phase when setup to approximately measure 0 g. Figure 11 shows the correlation coefficient and slope between the IP and OOP channels for the same experiments. Between the two measurement setups, the phase for maximum IP scale factor shifted by about 5.340° and the phase for a slope of -1 shifted by about 1.645°. Thus tracking information related to the OOP channel can provide a simple means to adjust the phase reference.

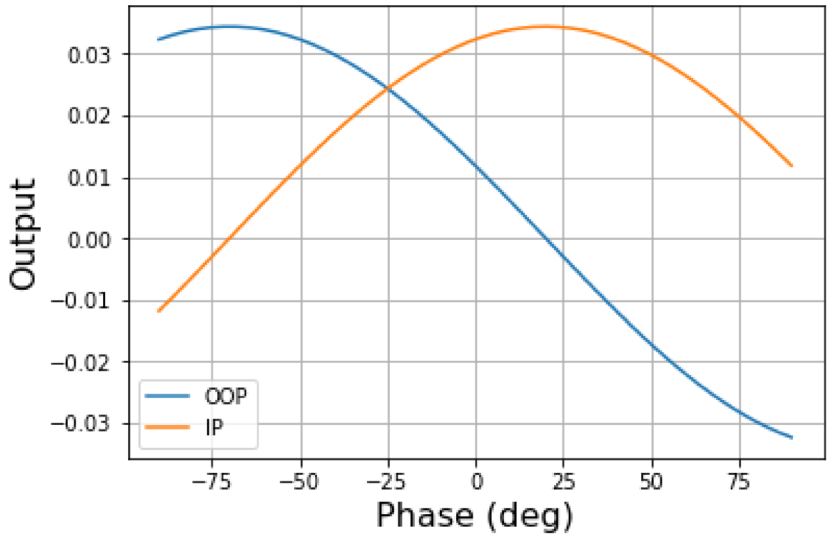

Figure 10. The mean value of the IP and OOP channels versus phase when setup to measure about 0 g.

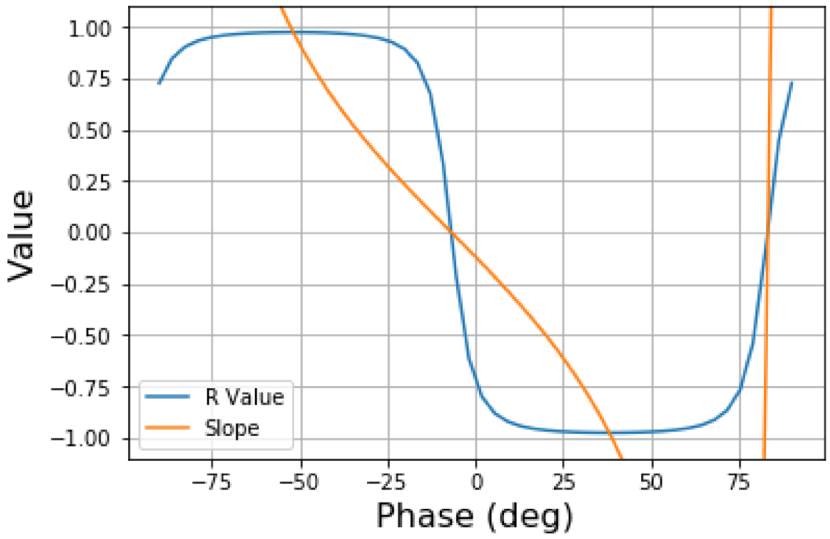

Figure 11. The correlation coefficient and slope between the IP and OOP channels versus phase when setup to measure about 0 g. A slope of -1 occurs for a phase of 37.379°.

Figure 12 shows the IP response to about a 0 g input with the phase reference selected such that the slope between the IP and OOP channels is -1. As before, to quantify the various noise processes that impact each response, the Allan deviation of the time series are shown in Figure 13. Again, while the uncompensated response slowly drifts, the compensated response does not. However, after an averaging time of 100 sec, unlike the -1 g response, the output is described by a 1/f noise process. As feedback has been expected to be needed to remove some nonlinearities in the system [4] and shown to be important to address issues related to shock and vibration [7], this preliminary work demonstrates that operating around different in-phase displacement states may provide improvements to stability. The 0 g measurement state is also much more sensitive to the vibrations of the pump used to evacuate the vacuum chamber, so this 1/f noise could be related to this.

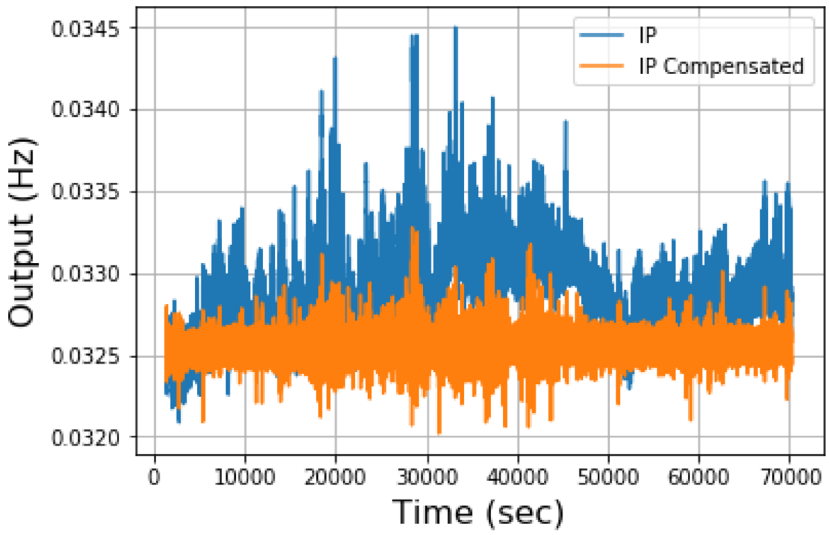

Figure 12. Time series of the IP and IP channel compensated with the OOP channel when setup to measure about 0 g. The mean and standard deviation of the IP compensated response is 3.256×10^{-2} +/- 0.005×10^{-2} Hz.

To help display the differences in noise processes associated with the two measurements setups, Figure 14 shows the Allan deviation scaled to g's. Assuming that the estimate for bias instability from the 0 g measurement is degraded by pump vibrations, the best estimate for bias instability comes from the the -1 g measurement of 1.34 μg. The test associated with measuring -1 g was stopped short due to a lack of available memory on the Red Pitaya, so it is very possible that the bias instability is lower. Future work will assess this.

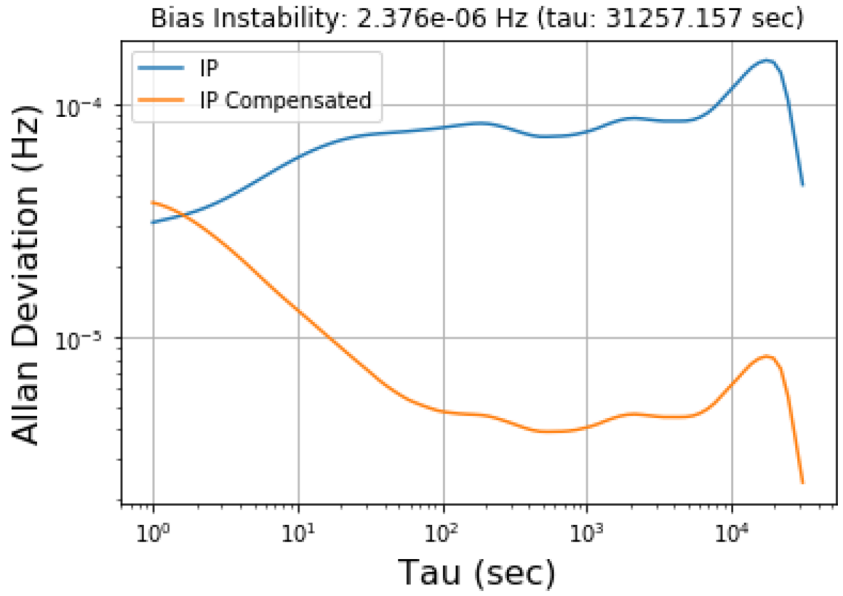

Figure 13. Allen deviation of the IP and IP channel compensated with the OOP channel when setup to measure about 0 g.

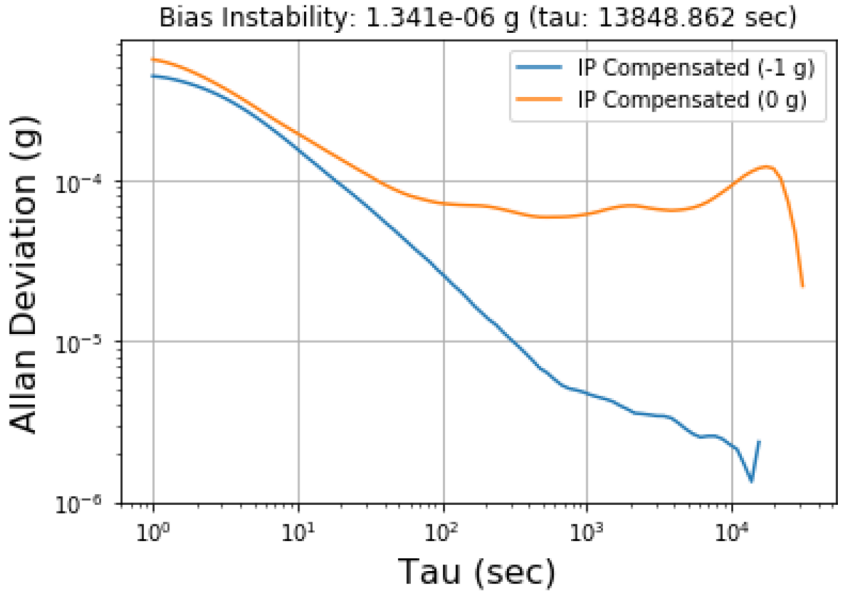

Figure 14. Allen deviation of the IP compensated responses to about 0 g and -1 g inputs scaled to g's.

5. CONCLUSIONS AND FUTURE EFFORTS

Building upon prior work, this report documents a novel means to select the offset phase for the phase reference for FM accelerometers. An overview of the current or accepted approach to select the offset phase is discussed. In experiments, it was found that the IP and OOP channels are highly correlated. Using this information, a simple approach to select the offset phase was presented. This approach can also be used to improve long-term stability and remove the need for autoregressive modeling used in prior work. At the longest integration times, bias instability is improved by more than two orders of magnitude. However, as the Allan deviation at the longest integration times is not limited by long-term drift or 1/f noise, the bias instability is expected to be lower.

In regards to future work, planned experiments will include testing for longer periods of time to measure the minimum bias instability. The source of drift related to the uncompensated response has not be conclusively identified, but experiments with the same analog automatic gain control circuit applied to FM gyroscopes found that the amplitude would exhibit similar drift (see [8] for examples of amplitude drift from the same circuit when applied to an FM gyroscope). Experiments with a digital automatic gain control circuit were able to address this long-term amplitude drift. As for improving the resolution of the sensor, work is currently in progress to increase the resolution of the frequency detector. New resonators that could be used to implement lower phase noise oscillators are being fabricated. These resonators also have a much lower in-phase natural frequency, so the scale factor is expected to be much higher at the same bias voltage. To push beyond capacitive detection, experiments related to optical detection have been planned.

This page is intentionally blank.

REFERENCES

1. Needham, T. G. and Braasch, M. S. 2017. "Impact of gravity modeling error on integrated GNSS/INS coasting performance," *36th IEEE/AIAA Digital Avionics Systems Conference (DASC 2017)*, URL https://doi.org/10.2514/6.1977-1081.

2. Jekeli, C. 2006. "Precision Free-Inertial Navigation with Gravity," *Journal of Guidance, Control, and Dynamics*, vol. 29, no. 3, pp. 704–713.

3. Richeson, J. A. and Pines, D. J. 2007. "GPS Denied Inertial Navigation Using Gravity Gradiometry," *AIAA Guidance, Navigation and Control Conference and Exhibit*, URL https://doi.org/10.2514/6.2007-6791.

4. Sabater, A. B., Bozeman, E., and Hobbs, S. 2022. "Towards Real-Time Accelerometer Bias Calibration: FY21 Status Update for Strapdown Gravity Aided Inertial Navigation System (GAINS)," Tech. Rep. TR-3263, Naval Information Warfare Center Pacific.

5. Kaajakari, V., Koskinen, J. K., and Mattila, T. 2007. "Phase noise in capacitively coupled micromechanical oscillators," *IEEE Transactions on Ultrasonics, Ferroelectrics, and Frequency Control*, vol. 52, no. 12, pp. 2322–2331.

6. Sabater, A. B., Bozeman, E., Horta, O., Moran, K. M., and Stanzione, K. 2020. "Quantization Requirements for FM Gyroscopes An Update on the Nonlinear FM Gyroscope," *2020 Joint Conference of the IEEE International Frequency Control Symposium and International Symposium on Applications of Ferroelectrics (IFCS-ISAF)*, URL https://doi.org/10.1109/IFCS-ISAF41089.2020.9234859.

7. Pagani, L. G., Frigerio, P., Falato, D., Padovani, C., Rizzini, F., and Langfelder, G. 2022. "Active Shock/Vibes Rejection in FM MEMS Accelerometers," *9th IEEE International Symposium on Inertial Sensors and Systems (Inertial 2022)*.

8. Sabater, A. B. 2022. "An Empirical Study on the Drift Mechanisms of Lissajous FM Gyroscopes: Amplitude, Frequency and Temperature Control," Tech. Rep. TR-TBD, Naval Information Warfare Center Pacific.

This page is intentionally blank.

INITIAL DISTRIBUTION

84310	Technical Library/Archives	(1)
71780	A. Sabater	(1)

Defense Technical Information Center
Fort Belvoir, VA 22060–6218 (1)

This page is intentionally blank.

REPORT DOCUMENTATION PAGE

Form Approved
OMB No. 0704-01-0188

PLEASE DO NOT RETURN YOUR FORM TO THE ABOVE ADDRESS.

1. REPORT DATE *(DD-MM-YYYY)*	2. REPORT TYPE	3. DATES COVERED *(From - To)*
July 2022	Final	

4. TITLE AND SUBTITLE

Quadrature Compensation and Demodulation Phase Reference Selection for FM Accelerometers

5a. CONTRACT NUMBER

5b. GRANT NUMBER

5c. PROGRAM ELEMENT NUMBER

6. AUTHORS

Andrew Sabater
NIWC Pacific

5d. PROJECT NUMBER

5e. TASK NUMBER

5f. WORK UNIT NUMBER

7. PERFORMING ORGANIZATION NAME(S) AND ADDRESS(ES)

NIWC Pacific
53560 Hull Street
San Diego, CA 92152–5001

8. PERFORMING ORGANIZATION REPORT NUMBER

TR- 3284

9. SPONSORING/MONITORING AGENCY NAME(S) AND ADDRESS(ES)

The NIWC Pacific In-House Laboratory Independent Research
53560 Hull Street
San Diego, CA 92152–5001

10. SPONSOR/MONITOR'S ACRONYM(S)

ILIR

11. SPONSOR/MONITOR'S REPORT NUMBER(S)

12. DISTRIBUTION/AVAILABILITY STATEMENT

DISTRIBUTION STATEMENT A. Approved for public release: distribution unlimited

13. SUPPLEMENTARY NOTES

Inertial navigation; FM; orthogonal channels

14. ABSTRACT

Inertial navigation provides a means to operate independent of external signals such as the ones provided by a GNSS (global navigation satellite system). The estimated position provided by inertial navigation will drift for a variety of reasons internal and external to the utilized sensors, but removing bias drift from the accelerometers can significantly mitigate this issue. This work aims to address this issue. The methods described herein document means to select the offset phase of frequency modulated (FM) accelerometers that can both be implemented in a real-time fashion and be used with a simple model to improve long-term stability. It provides improvements upon prior work that utilized autoregressive modeling, so this method is expected to be suitable for nonstationary acceleration. The method is based on an observation in experiments that found orthogonal channels to be highly correlated. Utilizing this approach, bias instability was improved by more than two orders of magnitude. However, as the bias instability was recorded at the longest measurement period, by increasing the measurement length, it is expected that the actual bias instability is lower. Future work to determine this as well as other areas are outlined at the end of the report.

15. SUBJECT TERMS

Internal navigation; orthogonal channels method

16. SECURITY CLASSIFICATION OF:			17. LIMITATION OF ABSTRACT	18. NUMBER OF PAGES	19a. NAME OF RESPONSIBLE PERSON
a. REPORT	b. ABSTRACT	c. THIS PAGE			Andrew Sabater
U	U	U	SAR	30	19B. TELEPHONE NUMBER *(Include area code)* 619-553-2480

This page is intentionally blank.

This page is intentionally blank.

Naval Information Warfare Center Pacific (NIWC) Pacific
San Diego, CA 92152-5001